

Thermal transport of the XXZ chain in a magnetic field

F. Heidrich-Meisner,^{1,*} A. Honecker,¹ and W. Brenig¹

¹*Technische Universität Braunschweig, Institut für Theoretische Physik,
Mendelssohnstrasse 3, 38106 Braunschweig, Germany*

(Dated: February 15, 2005)

We study the heat conduction of the spin-1/2 XXZ chain in finite magnetic fields where magnetothermal effects arise. Due to the integrability of this model, all transport coefficients diverge, signaled by finite Drude weights. Using exact diagonalization and mean-field theory, we analyze the temperature and field dependence of the thermal Drude weight for various exchange anisotropies under the condition of zero magnetization-current flow. First, we find a strong magnetic field dependence of the Drude weight, including a suppression of its magnitude with increasing field strength and a non-monotonic field-dependence of the peak position. Second, for small exchange anisotropies and magnetic fields in the massless as well as in the fully polarized regime the mean-field approach is in excellent agreement with the exact diagonalization data. Third, at the field-induced quantum critical line between the para- and ferromagnetic region we propose a universal low-temperature behavior of the thermal Drude weight.

I. INTRODUCTION

Transport properties of one-dimensional spin-1/2 systems are currently at the focus of active research. This has been motivated by the experimental manifestation of significant contributions to the thermal conductivity originating from magnetic excitations^{1,2,3,4,5,6}, stimulating intensive theoretical work^{7,8,9,10,11,12,13,14,15,16,17,18,19}. Strong theoretical efforts^{7,8,9,10,11,13,14} have been devoted to the question of possible ballistic thermal transport in generic spin models such as spin ladders, frustrated chains, and dimerized chains. Such ballistic transport would be characterized by a finite thermal Drude weight. Recent numerical and analytical studies indicate that in pure but *nonintegrable* spin models, the thermal Drude weight scales to zero in the thermodynamic limit implying that the thermal current is likely to have a finite intrinsic life-time^{8,9,12,13,14}. In addition, the effects of extrinsic magnon scattering by phonons and/or impurities have been addressed in several works^{10,12,15}. For the integrable XXZ model, the energy current operator is a conserved quantity^{20,21}, leading to a finite thermal Drude weight. Its temperature dependence has been studied with exact diagonalization^{7,8,9} and Bethe ansatz techniques^{16,17} and is well understood for arbitrary values of the exchange anisotropy at zero magnetic field. In this paper, we address the issue of thermal transport in the XXZ model in the presence of a finite magnetic field h . In this case, magnetothermal effects become important and must be accounted for. The magnetothermal response itself has been studied by Louis and Gros in the limit of small magnetic fields¹⁸ and recently also by Sakai and Klümper in the low-temperature limit¹⁹. Here, we consider magnetic fields of arbitrary strength and we discuss the temperature dependence of the thermal Drude weight under the condition of zero spin-current flow.

The Hamiltonian of the XXZ model reads

$$H = J \sum_{l=1}^N \left\{ \frac{1}{2} (S_l^+ S_{l+1}^- + \text{H.c.}) + \Delta S_l^z S_{l+1}^z - h S_l^z \right\} \quad (1)$$

where N is the number of sites, $S_l^{z,\pm}$ are spin-1/2 operators acting on site l , and Δ denotes the exchange anisotropy. The exchange coupling J is set to unity in our numerical calculations. We focus on $\Delta \geq 0$ and periodic boundary conditions are imposed.

The quantum phases and the spectrum of (1) are well understood, both as a function of exchange anisotropy Δ and magnetic field h . The reader is referred to Ref. 22 for a detailed summary and further references. Here we only repeat the main points. At zero magnetic field, the spectrum of the Hamiltonian Eq. (1) is gapless for $|\Delta| \leq 1$ and gapped for $|\Delta| > 1$. The situation at finite magnetic fields is summarized in the first four columns of Table I. Three different cases are found: (i) the ferromagnetic gapped state for $h > h_{c2} = 1 + \Delta$ (FM); (ii) the gapless or massless phase for $h < h_{c2} = 1 + \Delta$ and $h > h_{c1}$; and (iii) the antiferromagnetic, gapped state for $\Delta > 1$ and $h < h_{c1}$ (AFM). The line $h = h_{c1}$ starts at the $SU(2)$ symmetric point $\Delta = 1, h = 0$ and h_{c1} grows exponentially slowly in the region $\Delta > 1, h > 0$.

		h	m_0	$T/J \ll 1$
(i)	FM, gap	$h > h_{c2}$	1/2	$K_{\text{th}} \propto T^{3/2} \exp(-G/T)$
	Saturation	$h = h_{c2}$	1/2	$K_{\text{th}} = \text{const } T^{3/2}$
		$h_{c2} = 1 + \Delta$		
(ii)	Massless	$h_{c1} < h < h_{c2}$		$K_{\text{th}} \propto T$
(iii)	AFM, gap	$h < h_{c1}$	0	

TABLE I: Magnetic phases of the XXZ model (see, e.g., Ref. 22) and leading term of the thermal Drude weight K_{th} at low temperatures. m_0 is the average local magnetization at $T = 0$. $G = G(h)$ denotes the gap in either the polarized state (i) or the massive antiferromagnetic regime (iii). In the polarized state (i), $G(h)/J = h - h_{c2}$.

The fifth column of Table I is a first account of our main findings for the low-temperature behavior of the thermal Drude weight, denoted by K_{th} in this paper. These results are now briefly summarized. One can expect qualitative changes in the low-temperature behavior of the thermal Drude weight as the transition lines $h = h_{c1}$ and $h = h_{c2}$ are crossed. In particular, we focus on the transition from the gapless phase to the ferromagnetic state. In Sec. III, we will argue that for $T/J \ll 1$, first, $K_{\text{th}} \propto T^{3/2} \exp(-G/T)$ in the ferromagnetic state, G being the gap, and T temperature; second, $K_{\text{th}} \propto T$ in the massless phase; and third, $K_{\text{th}} \propto T^{3/2}$ along the line $h = h_{c2}$.

Regarding the antiferromagnetic state, there is certainly also an exponentially suppressed Drude weight; see for instance Refs. 8 and 17 for $h = 0$. However, the low-temperature region in this case and for $h = h_{c1}$ is difficult to reach with the methods of the present paper. For a discussion of the low-temperature limit at vanishing magnetic field, we refer the reader to Refs. 8,9,16 and 17. Apart from the low-temperature behavior, this paper studies the field dependence of the thermal Drude weight in the phases (i) and (ii) at finite temperatures.

The plan of this paper is the following. First, we discuss the expressions for the transport coefficients and the current operators in Sec. II. Second, in Sec. III we perform an analysis of the transport coefficients based on a Jordan-Wigner mapping of the spin system onto spinless fermions. In this case, interactions at $\Delta \neq 0$ will be treated by a Hartree-Fock approximation. Third, we present our results from exact diagonalization for $\Delta > 0$ in Sec. IV and compare them to the results from the Jordan-Wigner approach. The field and temperature dependence of the thermal Drude weight is discussed with a particular focus on the case of the Heisenberg chain. A summary and conclusions are given in Sec. V.

II. TRANSPORT COEFFICIENTS

Within linear response theory, the thermal and the spin current are related to the gradients ∇h and ∇T of the field h and the temperature T by²³

$$\begin{pmatrix} J_1 \\ J_2 \end{pmatrix} = \begin{pmatrix} L_{11} & L_{12} \\ L_{21} & L_{22} \end{pmatrix} \begin{pmatrix} \nabla h \\ -\nabla T \end{pmatrix} \quad (2)$$

where $J_i = \langle j_i \rangle$ is either the thermodynamic expectation value of the spin current j_1 or the thermal current operator j_2 , respectively. L_{ij} denote the transport coefficients. At finite frequencies ω , the coefficients $L_{ij}(\omega)$ depend on the time-dependent current-current correlation functions via²³

$$L_{ij}(\omega) = \frac{\beta^r}{N} \int_0^\infty dt e^{i(-\omega+i0^+)t} \int_0^\beta d\tau \langle j_i j_j(t+i\tau) \rangle. \quad (3)$$

In this equation, $r = 0$ for $j = 1$ and $r = 1$ for $j = 2$. $\beta = 1/T$ is the inverse temperature and $\langle \cdot \rangle$ denotes the thermodynamic expectation value. Note that

$L_{12} = L_{21}/T$ due to Onsager's relation²³. The real part of $L_{ij}(\omega)$ can be decomposed into a δ -function at $\omega = 0$ with weight D_{ij} and a regular part $L_{ij}^{\text{reg}}(\omega)$:

$$\text{Re } L_{ij}(\omega) = D_{ij} \delta(\omega) + L_{ij}^{\text{reg}}(\omega). \quad (4)$$

This equation defines the Drude weights D_{ij} , for which a spectral representation can be given²¹

$$D_{ij}(h, T) = \frac{\pi \beta^{r+1}}{N} \sum_{\substack{m, n \\ E_m = E_n}} p_n \langle n | j_i | m \rangle \langle m | j_j | n \rangle. \quad (5)$$

Here, $p_n = \exp(-\beta E_n)/Z$ is the Boltzmann weight and Z denotes the partition function. In the exponent, r has to be chosen in the same way as in Eq. (3).

Let us now introduce the appropriate definitions of the current operators. The local current operators $j_{1,l}$ and $j_{2,l}$ satisfy the continuity equations

$$j_{j,l+1} - j_{j,l} = -i[H, d_{j,l}]; \quad j = 1, 2 \quad (6)$$

where $d_{1,l} = S_l^z$ is the local magnetization density and $d_{2,l} = h_l$ is the local energy density, respectively, with $H = \sum_l h_l$. At zero magnetic field, the total currents $j_{\text{th}[s]} = \sum_l j_{\text{th}[s],l}$ are given by^{21,24,25}

$$j_s = iJ \sum_{l=1}^N (S_l^+ S_{l+1}^- - S_{l+1}^+ S_l^-) \quad (7)$$

$$j_{\text{th}} = J^2 \sum_{l=1}^N \tilde{S}_l \cdot (\tilde{S}_{l+1} \times \tilde{S}_{l+2}) \quad (8)$$

with the definition $\tilde{S}_l = (S_l^x, S_l^y, \Delta S_l^z)$ to achieve a compact representation, while \vec{S}_l is defined as usual. Note that subscripts in brackets $[\cdot]$ refer to spin transport.

At finite magnetic field, the proper set of current operators is¹⁸

$$j_1 = j_s; \quad j_2 = j_{\text{th}} - h j_s. \quad (9)$$

Now, the crucial point is that, while the *spin* current j_s is only conserved in the XX case ($\Delta = 0$), the current j_{th} is conserved for all fields h and values of Δ , i.e., $[H, j_{\text{th}}] = 0$ (Refs. 20 and 21). Thus, it immediately follows from Eqs. (3) and (9) that the Drude weights D_{12} , D_{21} , and D_{22} are finite for arbitrary fields h .

Furthermore, one can show that the spin Drude weight D_{11} is also finite in the thermodynamic limit for $h \neq 0$. We briefly outline the proof along the lines of Ref. 21. Given a set of all conserved observables $\{Q_l\}$, the spin Drude weight D_{11} can be written as

$$D_{11}(h, T) = \frac{\pi}{TN} (j_1 | \mathcal{P} j_1) \quad (10)$$

where \mathcal{P} is the projection operator in the Liouville space on the subspace spanned by all conserved quantities $\{Q_l\}$. The brackets $(\cdot | \cdot)$ denote Mori's scalar product;

see, e.g., Ref. 26 for details. Restricting to a subset $\{Q_m\} \subset \{Q_l\}$, one obtains an inequality^{21,27}

$$D_{11}(h, T) \geq \frac{\pi}{TN} \sum_m \frac{\langle j_1 Q_m \rangle^2}{\langle Q_m^2 \rangle}, \quad (11)$$

providing a lower bound for the Drude weight $D_{11}(h, T)$. In the literature, this relation is often referred to as Mazur's inequality^{21,27}. Several authors^{21,28} have used Eq. (11) to infer a finite spin Drude weight for the Heisenberg chain, assuming broken particle-hole symmetry, or the presence of a finite magnetic field, respectively. More explicitly, only one conserved quantity is often considered in Eq. (11), namely $Q_1 = j_{\text{th}}$, which has a finite overlap $\langle j_1 | j_{\text{th}} \rangle > 0$ with the spin current for $h \neq 0$. This finally proves $D_{11}(h, T) > 0$ for $h \neq 0$.

The main focus of this paper is on the case of purely thermal transport with a vanishing spin current, i.e., $J_1 = 0$. We therefore arrive at a thermal conductivity κ which is described by

$$\text{Re } \kappa(\omega) = K_{\text{th}}(h, T) \delta(\omega) + \kappa_{\text{reg}}(\omega) \quad (12)$$

where $K_{\text{th}}(h, T)$ in terms of the Drude weights D_{ij} reads

$$K_{\text{th}}(h, T) = D_{22}(h, T) - \beta \frac{D_{21}^2(h, T)}{D_{11}(h, T)}. \quad (13)$$

Exactly the same result for $K_{\text{th}}(h, T)$ is obtained if a different choice of current operators and corresponding forces is made, e.g., j_s and j_{th} from Eqs. (7) and (8) (see Ref. 23). The expression for $K_{\text{th}}(h, T)$, being fully equivalent to Eq. (13), is then given by

$$K_{\text{th}}(h, T) = D_{\text{th}}(h, T) - \beta \frac{D_{\text{th},s}^2(h, T)}{D_s(h, T)}. \quad (14)$$

Note that for $h = 0$, $K_{\text{th}}(h = 0, T) = D_{\text{th}}(h = 0, T)$. Therefore, two competing terms contribute to $K_{\text{th}}(h, T)$ in Eq. (14): the "pure" thermal Drude weight D_{th} and the "magneto-thermal correction", $\beta D_{\text{th},s}^2 / D_s$. Note that the magneto-thermal correction might be suppressed by external scattering or spin-orbit coupling, breaking the conservation of the total magnetization of the spin system (Ref. 12). This is an open issue which may depend crucially on the particular material investigated in experimental transport studies.

Let us now give spectral representations for the quantities $D_s(h, T)$, $D_{\text{th}}(h, T)$, and $D_{\text{th},s}(h, T)$ (Refs. 21,29,30)

$$D_{\text{th}[s]}^I(h, T) = \frac{\pi \beta^2 [1]}{N} \sum_{\substack{m,n \\ E_m = E_n}} p_n |\langle m | j_{\text{th}[s]} | n \rangle|^2, \quad (15)$$

$$D_s^{II}(h, T) = \frac{\pi}{N} \left[\langle -\hat{T} \rangle - 2 \sum_{\substack{m,n \\ E_m \neq E_n}} p_n \frac{|\langle m | j_s | n \rangle|^2}{E_m - E_n} \right], \quad (16)$$

$$D_{\text{th},s}(h, T) = \frac{\pi \beta}{N} \sum_n p_n \langle n | j_{\text{th}} j_s | n \rangle. \quad (17)$$

The operator $\hat{T} = (1/2) \sum_l (S_l^+ S_{l+1}^- + \text{H.c.})$ is the kinetic energy. In the Eqs. (15), (16), and (17), the magnetic field only enters via the Boltzmann weights p_n . The two expressions D_s^I and D_s^{II} are equivalent in the thermodynamic limit, but exhibit differences at low temperatures for finite system sizes^{21,31,32,33,34}. In this context, note that $D_s^{II} - D_s^I$ is the so-called Meissner fraction, which measures the *superfluid* density in the thermodynamic limit and in a transverse vector-field^{32,33}. This quantity vanishes for $N \rightarrow \infty$ in one dimension, but it can be nonzero for finite systems³³. In Ref. 9, we have performed a study of the finite-size scaling of both quantities for the XXZ chain, showing that $D_s^I \approx D_s^{II}$ already holds at sufficiently high temperatures. At low temperatures and zero magnetic field, D_s^I is always exponentially suppressed for even N due to finite-size gaps; thus a finite value of $D_s(T = 0)$ can only be found for $N \rightarrow \infty$. On the contrary, since $D_s^{II} \approx (\pi/N) \langle -\hat{T} \rangle$ at low temperatures, D_s^{II} correctly results in a *finite* value at $T = 0$ in the massless regime. Depending on the context, one should carefully check which of these two quantities exhibits the more reliable finite-size behavior, and in fact, in the present case of finite magnetic fields we will argue in Sec. IV that D_s^I should preferably be used. For a more detailed discussion of the relation between D_s^I and D_s^{II} , we refer the reader to Ref. 9 and references therein.

In our numerical analysis, we will evaluate D_{th} , D_s , and $D_{\text{th},s}$ while the coefficients D_{ij} from Eq. (13) can be derived if desired as they are linear combinations of D_{th} , D_s , and $D_{\text{th},s}$:

$$D_{11} = D_s, \quad (18)$$

$$D_{21} = D_{\text{th},s} - h D_s, \quad (19)$$

$$D_{22} = D_{\text{th}} - 2\beta h D_{\text{th},s} + \beta h^2 D_s. \quad (20)$$

The XXZ model is integrable and solvable via the Bethe ansatz. Therefore one expects all quantities in Eqs. (13) and (14) to be accessible by analytical techniques. Yet, for the spin Drude weight $D_s(h = 0, T)$ at zero magnetic field, partly contradicting results can be found in the literature regarding both its temperature dependence and the question whether it is finite or not for the Heisenberg chain ($\Delta = 1$) in the thermodynamic limit. See Refs. 9,28,30,31,35,36,37,38 and further references therein.

III. MEAN-FIELD APPROXIMATION

We now discuss a Hartree-Fock type of approximation to the Hamiltonian Eq. (1), which we use to compute the Drude weights D_{ij} . The spin operators S_l^{\pm} are first mapped onto spinless fermions via the Jordan-Wigner transformation²³

$$S_l^z = c_l^\dagger c_l - \frac{1}{2}; \quad S_l^+ = e^{i\pi \Phi_l} c_l^\dagger. \quad (21)$$

Here, $c_l^{(\dagger)}$ destroys(creates) a fermion on site l . The string operator Φ_l reads $\Phi_l = \sum_{i=1}^{l-1} n_i$ with $n_i = c_i^\dagger c_i$. Next, the interaction term $\Delta n_l n_{l+1}$ appearing in the fermionic representation is treated by a Hartree-Fock decomposition leading to an effective mean-field Hamiltonian

$$H_{\text{MF}} = \sum_k \epsilon_k c_k^\dagger c_k \quad (22)$$

with the mean-field dispersion

$$\epsilon_k = -J\{(1 + 2\Delta\alpha) \cos(k) + h - 2\Delta(n - 1/2)\}. \quad (23)$$

The quantities to be determined self-consistently are $\alpha = \langle c_{l+1}^\dagger c_l \rangle$ and $n = \langle c_l^\dagger c_l \rangle$ where the latter is related to the average local magnetization m via $m = \langle S_l^z \rangle = n - 1/2$. The Drude weights can then be obtained from

$$D_{11} = (\pi\beta/N) \langle j_1^2 \rangle; \quad (24)$$

$$D_{21} = (\pi\beta/N) \langle j_2 j_1 \rangle; \quad (25)$$

$$D_{22} = (\pi\beta^2/N) \langle j_2^2 \rangle. \quad (26)$$

The current operators read

$$j_1 = \sum_k v_k c_k^\dagger c_k; \quad j_2 = \sum_k \epsilon_k v_k c_k^\dagger c_k$$

with $v_k = d\epsilon_k/dk$.

While this approach is exact for $\Delta = 0$, fair results for $K_{\text{th}}(h = 0, T)$ are even obtained for $0 < \Delta \leq 1$; see Refs. 8 and 9. From Eqs. (24) to (26), the leading contribution at low temperatures can be derived.

We start with the free fermion case $\Delta = 0$, for which we find at the saturation field h_{c2}

$$K_{\text{th}}(h, T) = \left(A_{22} - \frac{A_{21}^2}{A_{11}} \right) T^{3/2} \text{ for } h = h_{c2} \quad (27)$$

with

$$\begin{aligned} A_{11} &= \sqrt{\frac{\pi}{2}} (1 - \sqrt{2}) \zeta(1/2), \\ A_{21} &= \frac{3}{4} \sqrt{\frac{\pi}{2}} (2 - \sqrt{2}) \zeta(3/2), \\ A_{22} &= \frac{15}{16} \sqrt{\frac{\pi}{2}} (4 - \sqrt{2}) \zeta(5/2); \end{aligned} \quad (28)$$

$\zeta(x)$ being the Riemann-Zeta function. Note that the spin Drude weight at $T = 0$ is finite for $0 < h < h_{c2}$ and vanishes for $h \geq h_{c2}$. At low temperatures and for $h = h_{c2}$, we find $D_{11}(T) = A_{11} \sqrt{T}$ and a divergence of the pure thermal Drude weight D_{th} with $D_{\text{th}} \approx h_{c2}^2 A_{11} T^{-1/2}$ to leading order in temperature, which follows from Eqs. (19) and (20). We mention that the result $D_{22} \propto T^{3/2}$ at the critical field was also found within a continuum theory suggested to describe transport properties of two-leg spin ladders.¹⁰

In the intermediate regime, i.e., the gapless state (ii) [see Table I],

$$K_{\text{th}}(h, T) = \frac{\pi^2}{3} v(h) T; \quad v(h) = J \sqrt{1 - h^2} \quad (29)$$

holds at low temperatures, because the dispersion is linear in the vicinity of the Fermi level for $k_{\text{F}} \neq 0, \pi$. Note that $K_{\text{th}}(h, T) \approx D_{22}(h, T)$ for small T in this regime. Equation (29) results in $K_{\text{th}} = \pi^2 J T / 3$ for $h = 0$, which is, e.g., known from Ref. 16.

For $|h| > |h_{c2}| = 1$, both D_{22} and the second term in Eq. (13), i.e., $D_{21}^2 / (T D_{11})$, are given by

$$D_{22} = D_{21}^2 / (T D_{11}) = \sqrt{\frac{\pi}{2}} G^2 \frac{e^{-G/T}}{\sqrt{T}}, \quad (30)$$

to leading order in temperature and for $T \ll G$, where $G/J = |h| - 1$ is the gap. This implies that $K_{\text{th}}(h, T)$ is strongly suppressed at low temperatures due to the cancellation of the contributions to $K_{\text{th}}(h, T)$ in Eq. (13). In fact, such cancellation occurs in the next-to-leading order in T as well. One can further show, taking into account the first non-vanishing contribution to K_{th} in Eq. (13), that

$$K_{\text{th}}(h, T) = \frac{3}{4} \sqrt{2\pi} T^{3/2} e^{-G/T} \quad (31)$$

describes the low-temperature behavior of the thermal Drude weight above h_{c2} . In Ref. 10, it has been argued that $D_{22} \propto \exp(-G/T)/\sqrt{T}$ is a generic feature of gapped systems with a finite thermal Drude weight.

We further point out that the ratio of the thermal Drude weight K_{th} and the spin Drude weight D_s fulfills a Wiedemann-Franz type of relation in the low-temperature limit in all three cases, i.e., in the massless and the fully polarized state as well as for $h = h_{c2}$:

$$\frac{K_{\text{th}}}{D_s} = L_0 T. \quad (32)$$

The constant L_0 takes different values in the regimes (i) and (ii), but for the free-fermion case (and within mean-field theory as well) it is independent of the magnetic field *in* the massless and fully polarized state, respectively.

Before turning to the mean-field theory for $\Delta > 0$, let us briefly discuss which results can be expected from conformal field theory for the massless state. The expressions for the spin and thermal Drude weight D_{22} and D_{11} have the same structure as at zero magnetic field, i.e., $D_{22}(h, T) = (\pi^2/3) v(h, \Delta) T$ and $D_{11}(h, T) = K(h, \Delta) v(h, \Delta)$ with field-dependent velocity v and Luttinger parameter K (see, e.g., Refs. 8 and 9). This implies that the constant L_0 appearing in Eq. (32) is field dependent in the massless regime (see Ref. 16 for $h = 0$):

$$L_0 = \frac{\pi^2}{3 K(h, \Delta)}. \quad (33)$$

Furthermore, D_{21} vanishes in the continuum limit due to particle-hole symmetry. While a finite magnetic field initially breaks this symmetry for the original bosonic fields, the original form of the Luttinger-liquid Hamiltonian is restored by introducing a shifted bosonic field²². This

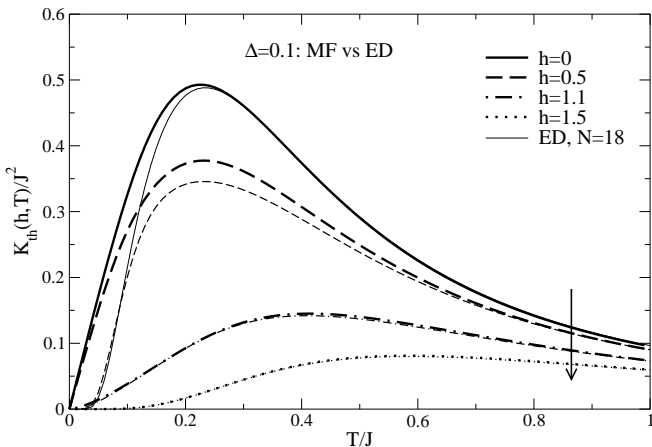


FIG. 1: Thermal Drude weight $K_{\text{th}}(h, T)$ of the XXZ chain for $\Delta = 0.1$: comparison of mean-field theory (MF) and exact diagonalization (ED). The thermal Drude weight $K_{\text{th}}(h, T)$ is shown for $h = 0, 0.5, 1.1, 1.5$. Increasing field is indicated by the arrow. Thick lines denote results from the Hartree-Fock approximation; thin lines: ED for $N = 18$. Deviations at low temperatures for $h = 0$ and $h = 0.5$ are due to finite-size effects in the ED results.

has an interesting consequence for the low temperature behavior of the pure thermal Drude weight D_{th} . Namely, by solving Eqs. (19) and (20) for D_{th} , one obtains

$$D_{\text{th}} = D_{22} + \frac{h^2 D_s}{T} = \frac{\pi^2}{3} v T + K v \frac{h^2}{T^{-1}}, \quad (34)$$

which implies that D_{th} diverges at low temperatures with T^{-1} in the massless regime, consistent with results of Ref. 19.

Additionally, one obtains K_{th} in the massless regime and in the low-temperature limit

$$K_{\text{th}}(h, T) \approx D_{22} = \frac{\pi^2}{3} v(h, \Delta) T. \quad (35)$$

Both parameters, i.e., $K = K(h, \Delta)$ and $v = v(h, \Delta)$, can be computed exactly by solving the Bethe-ansatz equations³⁹. The velocity $v = v(h)$ has been calculated for $\Delta = 1$ in Ref. 40. Further numerical values for these parameters can be found in, e.g., Ref. 41.

Let us next discuss the results from the mean-field approximation (MF) for $\Delta > 0$. Figure 1 shows $K_{\text{th}}(h, T)$ for $\Delta = 0.1$ and $h = 0, 0.5, 1.1, 1.5$ (thick lines). The main features are: (i) a suppression of the thermal Drude weight by the magnetic field; (ii) a shift of the maximum to higher temperatures for $h > 0.5$ compared to $h = 0$; (iii) a change in the low-temperature behavior which will be discussed in more detail below in this section.

For comparison, the results from exact diagonalization (ED) for $N = 18$ sites are included in Fig. 1 (thin lines) and we find that the agreement is very good. Deviations at low temperatures for $h = 0$ and $h = 0.5$ are due to finite-size effects, i.e., the ED results are not yet converged to the thermodynamic limit. For larger fields

$h \geq h_{c2} = 1.1$, deviations between ED and MF are negligibly small.

From Eq. (23), we can derive the critical field h_{c2} within the Hartree-Fock approximation. At $T = 0$ and $h = h_{c2}$, the ground state is the fully polarized state with $n = \langle c_i^\dagger c_i \rangle = 1$, i.e., the parameter α from Eq. (23) vanishes. Consequently, we find $h_{c2} = 1 + \Delta$ in accordance with the exact result²². Indeed, the low-energy theories along the line $h = 1 + \Delta$ and for $\Delta = 0$ are equivalent in the sense that they are characterized by the same Luttinger parameter^{39,42}. Within bosonization, the line $h = h_{c2}$ is particular since the velocity of the elementary excitations vanishes here.

Regarding the low-temperature behavior of the thermal Drude weight we can then conjecture that it is given by Eqs. (27) and (28) for $h = h_{c2}$, independently of Δ . We will come back to this issue in Sec. IV where we discuss the results from exact diagonalization for $\Delta > 0$. The case of $\Delta = -1$ and $h = 0$, however, seems to be an exception as we have found indications for $K_{\text{th}}(h = 0) \propto T$ at low temperatures before⁸. Here, the existence of many low-lying excitations might complicate the situation.

In the ferromagnetic state and for low temperatures, the parameter α from Eq. (23) is exponentially suppressed and the average local magnetization is $m = 1/2$. Thus, to leading order in T the low-temperature dependence of $K_{\text{th}}(h, T)$ is independent of Δ , similar to the case of $h = h_{c2}$, and the thermal Drude weight is exponentially suppressed $K_{\text{th}}(h, T) \propto T^{3/2} e^{-G/T}$ with $G = h - h_{c2}$.

In the gapless state our mean-field theory results confirm that $K_{\text{th}}(h, T) = V(h, \Delta) T$ for $\Delta > 0$ and low temperatures. However, the mean-field prefactor $V(h, \Delta)$ will be renormalized if interactions are fully accounted for; see Eq. (35).

In summary, we have obtained the leading low-temperature contributions to K_{th} in the regimes (i) and (ii) of Table I using mean-field theory and conformal field theory. Mean-field theory provides a reasonable quantitative description of the transport coefficients for small Δ and h as well as for $h \geq h_{c2}$.

IV. EXACT DIAGONALIZATION

In this section, we first present numerical results for the thermal Drude weight of the Heisenberg chain ($\Delta = 1$). Second, the field dependence of $K_{\text{th}}(h, T)$ for intermediate temperatures T is analyzed. Next, $K_{\text{th}}(h, T)$ for $h = h_{c2}$ is discussed for different choices of the anisotropy $\Delta \geq 0$ and finally, we make some remarks on the lower bound for the spin Drude weight $D_{11} = D_s$ given in Eq. (11). While $D_s(h, T)$ still eludes an exact analytical treatment for arbitrary temperatures, analytically exact results for $D_{\text{th}}(h, T)$ and $D_{\text{th},s}(h, T)$ of the Heisenberg chain have very recently been reported in Ref. 19.

Let us first address a technical issue, namely the ap-

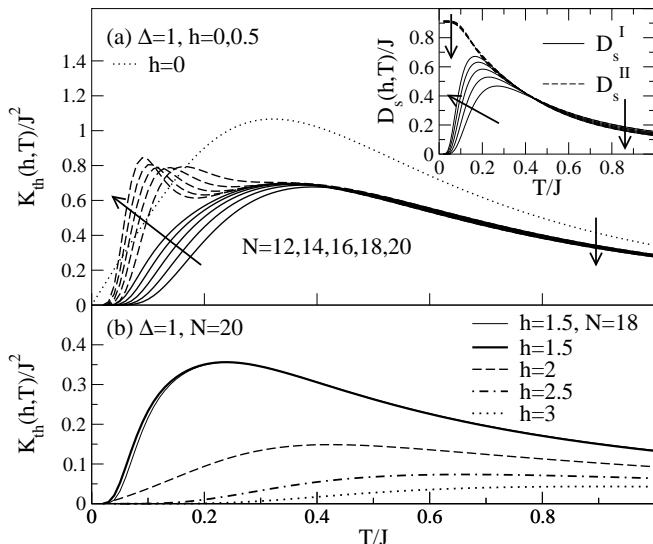


FIG. 2: Thermal Drude weight $K_{\text{th}}(h, T)$ of the Heisenberg chain ($\Delta = 1$). Panel (a): $K_{\text{th}}(h, T)$ computed from Eq. (14) using $D_s = D_s^I$ (solid lines) and $D_s = D_s^{II}$ (dashed lines), both for $h = 0.5$ and $N = 12, 14, 16, 18, 20$. Arrows indicate increasing system size. The dotted line is the result for $h = 0$ and $N \rightarrow \infty$ from Ref. 16. Inset: comparison of $D_s^I(h, T)$ [solid lines] and $D_s^{II}(h, T)$ [dashed lines]; $h = 0.5$, $\Delta = 1$. Panel (b): $K_{\text{th}}(h, T)$ for $h = 1.5, 2, 2.5, 3$ and $N = 20$ [thick lines; $D_s(h, T) = D_s^I(h, T)$]. The curve for $N = 18, h = 1.5$ is included (thin solid line).

appropriate choice for $D_s(h, T)$ in Eq. (14). For the case of zero magnetic field, we know from our previous study Ref. 9 that $D_s^I(h, T)$ and $D_s^{II}(h, T)$ exhibit a different finite-size behavior at $h = 0$. This is similar to the situation at finite fields. The inset of Fig. 2(a) shows both $D_s^I(h, T)$ and $D_s^{II}(h, T)$ for $\Delta = 1$ and $h = 0.5$, and we see that first, $D_s^{II}(h, T)$ is well converged at low temperatures; and second, a large difference between $D_s^I(h, T)$ and $D_s^{II}(h, T)$ is visible at low temperatures. The thermal Drude weight $K_{\text{th}}(h, T)$, resulting from either inserting $D_s^I(h, T)$ or $D_s^{II}(h, T)$ in Eq. (14), is shown in Fig. 2(a). We have decided to use D_s^I in the numerical study for consistency reasons, since then, all Drude weights entering in Eq. (14) have a similar finite-size dependence at low temperatures, characterized by the exponential suppression at low temperatures due to the finite-size gap. On the contrary, using $D_s^{II}(h, T)$ leads to an artificial double peak structure in $K_{\text{th}}(h, T)$; seen in Fig. 2(a).

We have checked that a similar scenario arises for $\Delta = 0$ for finite systems. However, for this case the Drude weight can be computed exactly in the thermodynamic limit and we find that one of the two maxima disappears. Thus we expect an analogous behavior for $\Delta > 0$, supporting the choice of D_s^I instead of D_s^{II} .

Further numerical results for $K_{\text{th}}(h, T)$ of the Heisenberg chain are provided in Fig. 2(b) for $h \geq 1.5$. The main features of the thermal Drude weight can be sum-

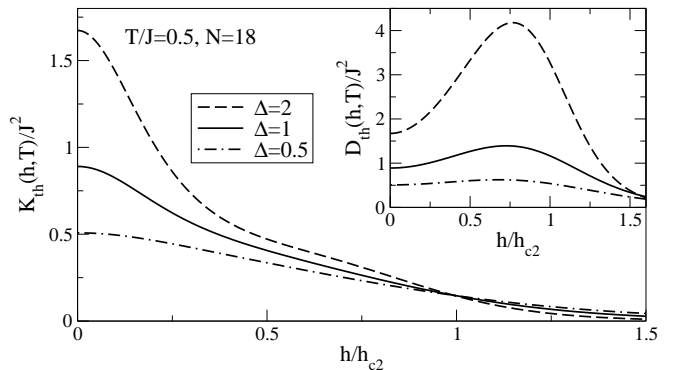


FIG. 3: Main panel: field dependence of the thermal Drude weight $K_{\text{th}}(h, T)$ for $\Delta = 0.5, 1, 2$ and $T/J = 0.5$ (ED for $N = 18$ sites). Inset: field dependence of $D_{\text{th}}(h, T)$ for the same parameter sets as in the main panel.

marized as follows: (i) for $0 < h < h_{c2}$, finite-size effects are small for $T/J \gtrsim 0.4$ [see Fig. 2(a)]; (ii) for $h \geq h_{c2}$, finite-size effects are negligible; (iii) the position of the maximum depends on the magnetic field; (iv) $K_{\text{th}}(h, T)$ is strongly suppressed as the magnetic field is increased.

As both $D_{\text{th}}(h, T)$ and $D_{\text{th},s}(h, T)$ converge rapidly to the thermodynamic limit at high temperatures, the small finite-size effects observed for $T/J \gtrsim 0.4$ [see Fig. 2(a)] are due to $D_s(h, T)$ [see the inset of Fig. 2(a)]. At low T , $K_{\text{th}}(h, T)$ increases with system size N while it decreases with growing N at high temperatures. The vanishing of pronounced finite-size effects upon approaching the line $h = h_{c2}$ from below can be ascribed to the fact that a description in terms of free fermions with parameters independent of Δ is valid here, as was already evidenced in the previous section. For the ferromagnetic state ($h > h_{c2}$), the curves shown in Fig. 2(b) for $N = 20$ are indistinguishable from the corresponding ones for $N = 18$ (not included in the figure) within the line width.

Regarding the position of the maximum, there is evidence that it is first shifted to higher temperatures when the field is switched on as compared to the case of $h = 0$; see Fig. 2(a). A precise determination of its position in the intermediate gapless phase is somewhat complicated as typically, the numerical data converge well down to roughly only the peak temperature. Still, there are indications that at strong fields $h \sim 1$, the maximum tends to be located at lower temperatures than for $h = 0$. This can be seen, for instance, in the case of $h = 1.5$ in Fig. 2(b). In the polarized state, $K_{\text{th}}(h, T)$ definitely peaks at larger temperatures than at vanishing field due to its exponential suppression at low temperatures.

The decrease of $K_{\text{th}}(h, T)$ as a function of increasing magnetic field as mentioned in the preceding discussion of the Heisenberg chain is also observed for other choices for the anisotropy Δ . This is demonstrated for $\Delta = 0.5, 1, 2$ at $T/J = 0.5$ in the main panel of Fig. 3, where $K_{\text{th}}(h, T)$ is shown as a function of the magnetic field h and plotted versus h/h_{c2} . In contrast to $K_{\text{th}}(h, T)$, $D_{\text{th}}(h, T)$ grows

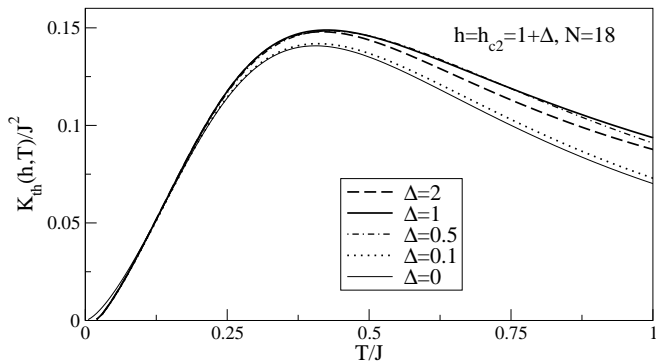


FIG. 4: Thermal Drude weight $K_{\text{th}}(h, T)$ at the critical field $h_{c2} = 1 + \Delta$ for $\Delta = 0, 0.1, 0.5, 1, 2$. For $\Delta \neq 0$, we show numerical results for $N = 18$ sites, while the curve for the free fermion case (thin solid line) is valid in the thermodynamic limit.

with increasing magnetic field at intermediate temperatures. For illustration, $D_{\text{th}}(h, T)$ is plotted versus h/h_{c2} at $T/J = 0.5$ in the inset of Fig. 3 for the same choice of parameters as in the main panel. It exhibits a maximum at large fields, which increases and its position approaches $h = h_{c2}$ when the temperature is lowered. Thus, indications of the transition to the ferromagnetic phase are visible in $D_{\text{th}}(h, T)$, but not present in $K_{\text{th}}(h, T)$. Note, however, that all three curves in the main panel of Fig. 3 almost pass through the same point for $h \approx h_{c2}$. For $T/J \lesssim 1$, $D_{\text{th}}(h, T)$ is enhanced by the magnetic field and we can therefore conclude that the decrease of $K_{\text{th}}(h, T)$ as a function of magnetic field is due to a cancellation of $D_{\text{th}}(h, T)$ and the magnetothermal correction in Eq. (14).

Along the critical line $h = h_{c2} = 1 + \Delta$, further evidence for universal low-temperature behavior can be found by ED. This can be seen in Fig. 4, where we present $K_{\text{th}}(h, T)$ for $\Delta = 0.1, 0.5, 1, 2$ and $N = 18$. The curve for $\Delta = 0$ is also included in the figure; this one, however, is exact in the thermodynamic limit. Below $T/J \approx 0.25$, the curves lie on top of each other. Small deviations at lowest temperatures visible in the plot can be ascribed to the presence of finite-size gaps. This supports our conclusion from Sec. III that Eqs. (27) and (28) hold for arbitrary $\Delta \geq 0$ and further numerical data (not included in the figure) show that it is also correct for $-1 < \Delta < 0$.

Finally, let us turn to the inequality Eq. (11) for the spin Drude weight $D_{11}(h, T) = D_s(h, T)$ introduced in Sec. II. Here, we want to discuss to which extent the inequality Eq. (11) is exhausted by j_{th} at finite magnetic fields and finite temperatures. An analogous analysis in the limit of $\beta = 0$ can be found in Ref. 21. To this end we compare $D_s^I(h, T)$ and

$$D_{\text{sub}}(h, T) := \frac{\pi}{TN} \frac{\langle j_s j_{\text{th}} \rangle^2}{\langle j_{\text{th}}^2 \rangle} = \frac{1}{T} \frac{D_{\text{th},s}^2(h, T)}{D_{\text{th}}(h, T)} \quad (36)$$

in Fig. 5. Note that first, the relation $D_s(h, T) \geq D_{\text{sub}}(h, T)$ is equivalent to the positivity of the ther-

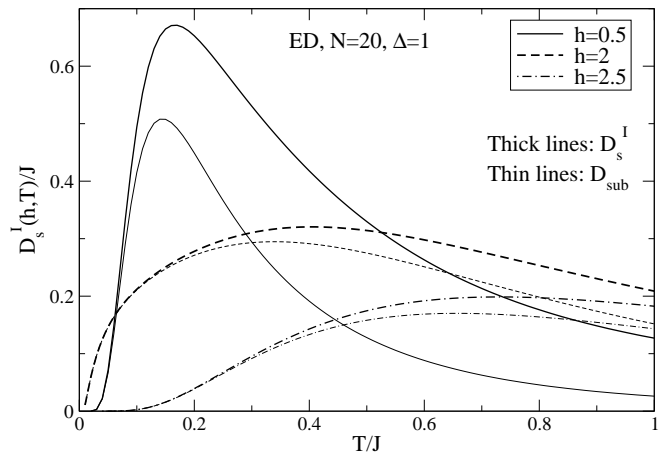


FIG. 5: Comparison of the spin Drude weight $D_s^I(h, T)$ (thick lines) and its lower bound D_{sub} (thin lines; see text for further details). The figure shows results for $\Delta = 1$, $N = 20$, and $h = 0.5, 2, 2.5$.

mal Drude weight $K_{\text{th}}(h, T) \geq 0$. Second, $D_s(h, T) \approx D_{\text{sub}}(h, T)$ implies a very small thermal Drude weight and thus, the comparison provided in Fig. 5 also reveals the relative size of the two contributions to $K_{\text{th}}(h, T)$ in Eq. (14), namely $D_{\text{th}}(h, T)$ and the magnetothermal correction $D_{\text{th},s}^2(h, T)/[T D_s^I(h, T)]$. In Fig. 5, results are shown for $\Delta = 1$, $N = 20$ sites, and $h = 0.5, 2, 2.5$. For the sake of clarity, data for smaller system sizes are not included in the figure. Differences between the curves for $N = 18$ and $N = 20$ are anyway only pronounced for temperatures $T/J \lesssim 0.1$ and become smaller as the magnetic field h increases.

Figure 5 allows for three major observations: (i) $D_s^I(h, T) \approx D_{\text{sub}}(h, T)$ at low temperatures and for all cases shown in the figure; (ii) $D_{\text{sub}}(h, T)$ approximates $D_s^I(h, T)$ the better the larger the magnetic field is; (iii) significant deviations are present for high temperatures implying that for a quantitative description of $D_s(h, T)$ using Eq. (11), more conserved quantities need to be considered in Eq. (11).

Our comparison provides, at least for finite system sizes, a quantitative measure of the temperature range where $D_s^I \approx D_{\text{sub}}$. Point (i) indicates that analytical approaches can make use of $D_{\text{sub}}(h, T)$ for a quantitative description of $D_s(h, T)$ at low temperatures as it has been done by Fujimoto and Kawakami within a continuum theory in Ref. 28. The quantities that appear on the right hand side of Eq. (36) are less involved than Eqs. (15) and (16) for $D_s(h, T)$, as the former are static correlators. Furthermore, for finite magnetic fields, we suggest to compute $D_s(h, T)$ analytically from Eq. (11), taking into account some of the conserved quantities Q_m , which are in principle known (see, e.g., Ref. 43). Such a procedure is applicable to $h \neq 0$ and might circumvent the ambiguities in the results encountered in recent computations of $D_s(h = 0)$ (Refs. 28,36,38,44). The latter have used Eq. (16) directly or Kohn's formula^{29,30},

equivalently. Regarding the relative size of $D_{\text{th}}(h, T)$ and the magnetothermal correction, we see that the latter becomes more relevant the larger the magnetic field is which leads to the strong suppression of $K_{\text{th}}(h, T)$. This is consistent with results of the previous sections of this paper.

V. CONCLUSIONS

In this paper we have studied the thermal Drude weight of the XXZ model with exchange anisotropy $\Delta \geq 0$ in finite magnetic fields using mean-field theory and exact diagonalization. Magnetothermal effects have been taken into account and the condition of zero magnetization current flow has been applied. Let us now summarize the main findings and relate them to experiments.

We have discussed the low-temperature limit of the thermal Drude weight $K_{\text{th}}(h, T)$ and we have given arguments that it changes from an algebraic behavior for $0 \leq \Delta \leq 1, h \leq h_{c2}$ to an exponentially activated behavior in the polarized state for $h > h_{c2}$. In addition, the leading term at low temperatures along the critical line $h = h_{c2}, \Delta > -1$, is universally given by $K_{\text{th}}(h, T) = AT^{3/2}$, where the prefactor A , given in Eqs. (27) and (28), is independent of Δ . In the gapless phase, the leading contribution to $K_{\text{th}}(h, T)$ is linear in the temperature with a field- and anisotropy dependent prefactor. In consequence, the thermal Drude weight $K_{\text{th}}(h, T)$ can be expected to be proportional to the specific heat in the gapless state in the low-temperature limit, where the velocity of elementary excitations is constant.

Further, the Drude weight is suppressed by the magnetic field, which can be ascribed to the increase of the magnetothermal correction relative to the pure thermal Drude weight $D_{\text{th}}(h, T)$. As a third result, the position of the maximum of $K_{\text{th}}(h, T)$ depends non-monotonically on the magnetic field. While in the present paper, we have focused on the thermal Drude weight K_{th} under the condition of zero spin-current flow, our analysis of the full transport matrix Eq. (2) can easily be extended to a variety of other transport situations, which would

be characterized by different combinations of the Drude weights.

Turning now to experiments, we emphasize that for a description of realistic materials external scattering has to be accounted for. In a simple picture, one may expect the Drude peak to be broadened by external scattering mechanisms. The behavior in magnetic fields that one may observe in experiments will likely depend both on external scattering rates as well as on the thermal Drude weight. Nevertheless, one may speculate that qualitative trends of the field dependence of the thermal Drude weight are reflected in thermal transport experiments.

In recent experiments on quasi one-dimensional magnetic materials^{1,2,3,4,5}, the thermal conductivity has often been found to be insensitive to the application of an external magnetic field. This is, however, explained by the large absolute value of the exchange coupling in these materials, being typically of the order of magnitude of 1000 K. It would therefore be desirable to perform measurements on materials with a moderately small exchange coupling to check our results. Still, it might be very difficult to reach the saturation field h_{c2} in realistic materials, but at least the qualitative features like the suppression of the thermal conductivity or a shift of the maximum could be verified. In particular, experiments in relatively large magnetic fields may provide an indirect probe of spin currents in one-dimensional quantum magnets, which have so far not yet been observed directly in experiments. Conclusions about the low-temperature limit would require reliable methods to separate the magnetic contribution from the phonon part, which is a challenging task in the interpretation of experiments. Nevertheless, we believe that further experiments on the field dependence of the thermal conductivity could hint at the nature and mechanisms of magnetic transport properties.

Acknowledgments - This work was supported by the DFG, Schwerpunktprogramm 1073. It is a pleasure to thank B. Büchner, D.C. Cabra, and C. Hess for fruitful discussions. We are indebted to C. Hess for a careful reading of the manuscript and valuable suggestions. We acknowledge support by the Rechenzentrum of the TU Braunschweig where parts of the numerical computations have been performed on a COMPAQ ES45.

* Electronic address: f.heidrich-meisner@tu-bs.de

¹ A.V. Sologubenko, K. Giannò, H.R. Ott, U. Ammerahl, and A. Revcolevschi, Phys. Rev. Lett. **84**, 2714 (2000).

² C. Hess, C. Baumann, U. Ammerahl, B. Büchner, F. Heidrich-Meisner, W. Brenig, and A. Revcolevschi, Phys. Rev. B **64**, 184305 (2001).

³ K. Kudo, S. Ishikawa, T. Noji, T. Adachi, Y. Koike, K. Maki, S. Tsuji, and Ken-ichi Kumagai, J. Phys. Soc. Jpn. **70**, 437 (2001).

⁴ A.V. Sologubenko, E. Felder, K. Giannò, H.R. Ott, A. Vitkine, and A. Revcolevschi, Phys. Rev. B **62**, R6108 (2000); A.V. Sologubenko, K. Giannò, H.R. Ott, A. Vi-

etkine, and A. Revcolevschi, *ibid.* **64**, 054412 (2001).

⁵ A.V. Sologubenko, H.R. Ott, G. Dhahlenne, and A. Revcolevschi, Europhys. Lett. **62**, 540 (2003).

⁶ C. Hess, H. ElHaes, B. Büchner, U. Ammerahl, M. Hücker, and A. Revcolevschi, Phys. Rev. Lett. **93**, 027005 (2004).

⁷ J.V. Alvarez and C. Gros, Phys. Rev. Lett. **89**, 156603 (2002); C. Gros and J.V. Alvarez, *ibid.* **92**, 069704 (2004).

⁸ F. Heidrich-Meisner, A. Honecker, D.C. Cabra, and W. Brenig, Phys. Rev. B **66**, 140406(R) (2002); Phys. Rev. Lett. **92**, 069703 (2004); J. Mag. Mag. Mat. **272-276**, 890 (2004).

⁹ F. Heidrich-Meisner, A. Honecker, D.C. Cabra, and

- W. Brenig, Phys. Rev. B **68**, 134436 (2003).
- ¹⁰ E. Orignac, R. Chitra, and R. Citro, Phys. Rev. B **67**, 134426 (2003).
- ¹¹ K. Saito, Phys. Rev. B **67**, 064410 (2003).
- ¹² E. Shimshoni, N. Andrei, and A. Rosch, Phys. Rev. B **68**, 104401 (2003).
- ¹³ X. Zotos, Phys. Rev. Lett. **92**, 067202 (2004).
- ¹⁴ F. Heidrich-Meisner, A. Honecker, D.C. Cabra, and W. Brenig, to appear in Physica B, cond-mat/0406378 (unpublished).
- ¹⁵ A.V. Rozhkov and A.L. Chernyshev, cond-mat/0407257 (unpublished).
- ¹⁶ A. Klümper and K. Sakai, J. Phys. A **35**, 2173 (2002).
- ¹⁷ K. Sakai and A. Klümper, J. Phys. A **36**, 11 617 (2003).
- ¹⁸ K. Louis and C. Gros, Phys. Rev. B **67**, 224410 (2003).
- ¹⁹ K. Sakai and A. Klümper, cond-mat/0410192 (unpublished).
- ²⁰ Th. Niemeijer and H.A. W. van Vianen, Phys. Lett. **34A**, 401 (1971).
- ²¹ X. Zotos, F. Naef, and P. Prelovšek, Phys. Rev. B **55**, 11029 (1997).
- ²² D.C. Cabra, A. Honecker, and P. Pujol, Phys. Rev. B **58**, 6241 (1998); D.C. Cabra and P. Pujol, *Field-Theoretical Methods in Quantum Magnetism*, Lect. Notes Phys. **645**, 253-305 (2004).
- ²³ G. D. Mahan, *Many-Particle Physics* (Plenum Press, New York, 1990).
- ²⁴ K. Kawasaki, Prog. Theor. Phys. **29**, 801 (1963).
- ²⁵ B.S. Shastry and B. Sutherland, Phys. Rev. Lett. **65**, 243 (1990).
- ²⁶ D. Forster, *Hydrodynamic Fluctuations, Broken Symmetry, and Correlation Functions* (Benjamin, Reading, Mass., 1975).
- ²⁷ P. Mazur, Physica **43**, 533 (1969); M. Suzuki, *ibid.* **51**, 277 (1971).
- ²⁸ S. Fujimoto and N. Kawakami, Phys. Rev. Lett. **90**, 197202 (2003).
- ²⁹ W. Kohn, Phys. Rev. **133**, A171 (1964).
- ³⁰ H. Castella, X. Zotos, and P. Prelovšek, Phys. Rev. Lett. **74**, 972 (1995).
- ³¹ B.N. Narozhny, A.J. Millis, and N. Andrei, Phys. Rev. B **58**, R2921 (1998); D.A. Rabson, B. N. Narozhny, and A.J. Millis, Phys. Rev. B **69**, 054403 (2004).
- ³² D. Scalapino, S.R. White, and S. Zhang, Phys. Rev. B **47**, 7995 (1993).
- ³³ T. Giamarchi, and B. S. Shastry, Phys. Rev. B **51**, 10915 (1995).
- ³⁴ S. Kirchner, H. G. Evertz, and W. Hanke, Phys. Rev. B **59**, 1825 (1999).
- ³⁵ X. Zotos and P. Prelovšek, Phys. Rev. B **53**, 983 (1996).
- ³⁶ X. Zotos, Phys. Rev. Lett. **82**, 1764 (1999).
- ³⁷ J.V. Alvarez and C. Gros, Phys. Rev. Lett. **88**, 077203 (2002); Phys. Rev. B **66**, 094403 (2002).
- ³⁸ M.W. Long, P. Prelovšek, S. El Shawish, J. Karadamoglou, and X. Zotos, Phys. Rev. B **68**, 235106 (2003).
- ³⁹ N.M. Bogoliubov, A.G. Izergin, and V.E. Korepin, Nucl. Phys. B **275**, 687 (1986); V.E. Korepin, N.M. Bogoliubov, and A.G. Izergin, *Quantum Inverse Scattering Method and Correlation Functions* (Cambridge University Press, Cambridge, England, 1993).
- ⁴⁰ P.R. Hammar, M.B. Stone, D.H. Reich, C. Broholm, P.J. Gibson, M.M. Turnbull, C.P. Landee, and M. Oshikawa, Phys. Rev. B **59**, 1008 (1999).
- ⁴¹ S. Qin, M. Fabrizio, Lu Yu, M. Oshikawa, and I. Affleck, Phys. Rev. B **56**, 9766 (1997).
- ⁴² G.I. Dzhaparidze and A.A. Nersesyan, JETP Lett **27**, 334 (1978); V.L. Pokrovsky and A.L. Talapov, Phys. Rev. Lett. **42**, 65 (1979).
- ⁴³ M.P. Grabowski and P. Matthieu, Ann. Phys. **243**, 299 (1996).
- ⁴⁴ A. Klümper, private communication.